Diffuse correlation spectroscopy: current status and future outlook

Stefan A. Carp⊙,* Mitchell B. Robinson⊙, and Maria A. Franceschini
Massachusetts General Hospital, Harvard Medical School,
Optics at Martinos Research Group, Charlestown, Massachusetts, United States

Abstract. Diffuse correlation spectroscopy (DCS) has emerged as a versatile, noninvasive method for deep tissue perfusion assessment using near-infrared light. A broad class of applications is being pursued in neuromonitoring and beyond. However, technical limitations of the technology as originally implemented remain as barriers to wider adoption. A wide variety of approaches to improve measurement performance and reduce cost are being explored; these include interferometric methods, camera-based multispeckle detection, and long path photon selection for improved depth sensitivity. We review here the current status of DCS technology and summarize future development directions and the challenges that remain on the path to widespread adoption. © *The Authors. Published by SPIE under a Creative Commons Attribution 4.0 International License. Distribution or reproduction of this work in whole or in part requires full attribution of the original publication, including its DOI.* [DOI: 10.1117/1.NPh.10.1.013509]

1 Introduction

Diffuse correlation spectroscopy (DCS) has emerged over the last decade as a versatile technique for noninvasive tissue perfusion measurements using near-infrared light.[1,2] As an extension of the dynamic light scattering technique[3] to multiply scattered light in tissue, DCS quantifies blood flow from the fluctuations in the intensity of diffusely scattered coherent light. The fluctuations result from the changing interference pattern at the detector due to moving tissue scatterers, a phenomenon primarily driven by red blood cell (RBC) movement.[4]

Typical DCS implementations use a long-coherence length laser for illumination and single mode fibers coupled to photon counting detectors to sample the intensity fluctuations of individual speckles on the tissue surface. The photon detection signals are then routed either to a hardware correlator or to a time-tagger that then streams the photon detection timestamps for postprocessing in the control computer using software autocorrelation algorithms. The fundamental DCS measurement is the normalized temporal intensity auto-correlation function $g_2(\tau) \equiv \frac{\langle I(t)I(t+\tau)\rangle}{\langle I(t)\rangle^2}$, where $I(t)$ is the measured light intensity and τ is the correlation lag time. In the majority of the work in the field so far, an analytical model based on the correlation diffusion equation[5] is then used to fit the measured g_2 and extract a blood flow index (BF$_i$). A key element in this process is choosing a motion model to link BF$_i$ with the scatterer mean square displacement: diffusion (random walk), $\langle \Delta r^2(\tau)\rangle = 6\mathrm{BF}_i\tau$, or convection (random flow), $\langle \Delta r^2(\tau)\rangle = \mathrm{BF}_i^2\tau^2$. Despite the apparent convective flow nature of RBC motion in vasculature, substantial experimental evidence indicates that a diffusive motion assumption for scatterer mean square displacement is needed for a good match of the DCS theoretical model with experimental data.[2] The shear-induced diffusion process[6] was proposed as an explanation, and simulations indicate that diffusive motion likely dominates DCS recordings under typical experimental conditions.[7] However, sensitivity to convective motion could be seen under certain conditions.[7–10]

Notwithstanding the remaining open questions on the origins of the DCS "signal," BF$_i$ has been shown to be reliably proportional to tissue blood flow through validation against a number

---

*Address all correspondence to Stefan A. Carp, stefan.carp@mgh.harvard.edu

of "gold-standard" techniques, including arterial spin-labeling magnetic resonance imaging (ASL-MRI),[11–13] fluorescent microspheres,[14] transcranial Doppler ultrasound (TCD),[15,16] xenon-enhanced computed tomography (Xe-CT),[17] bolus tracking time-domain near-infrared spectroscopy (NIRS),[18,19] phase-encoded velocity mapping MRI,[20] and $^{15}O_2$ positron emission tomography (PET).[21] Encouraged by these validation studies, a wide range of potential applications, primarily in neuromonitoring (see Refs. 1 and 22 for comprehensive reviews), but also in breast cancer,[23,24] muscle physiology[25–27] and animal models of diverse pathologies,[28–33] have been demonstrated. As seen in Fig. 1, the field has steadily grown over the past 15 years with more than 350 publications to date (this is an underestimate as some papers have been published under the name of "diffusing wave spectroscopy,"[34] the predicate technique for DCS in the soft matter physics field).

2 Benefits and Challenges

In addition to its intrinsic value as a noninvasive deep tissue perfusion monitoring method, DCS has several other beneficial characteristics. One is the simplicity of the hardware, consisting of just a few (admittedly expensive) components and a fully digital signal processing chain with no calibration or gain adjustments required. Further, because tissue driven intensity fluctuations are generally above 100 Hz, slow light intensity changes do not impact the recorded autocorrelations. As such, BF_i tends to return to the previous level after a motion artifact as long as overall contact is not lost, whereas a purely intensity-based measurement, as used in NIRS, for example, might show a significant step change in signal level.

Nevertheless, DCS in its standard implementation suffers from several significant challenges, some shared with NIRS (limited depth penetration, sensitivity to crosstalk from superficial physiology) and some specific to DCS (signal to noise ratio (SNR) limitations, difficulty in interpreting absolute BF_i values). Although the discussion below focuses on cerebral blood flow (CBF) monitoring, as the primary application area for DCS in the field, considerations of depth sensitivity and SNR are relevant to the full range of potential DCS applications.

To illustrate, Fig. 2(a) shows the distribution of the straight line distance between the scalp surface and gray matter in different areas of the head, derived from a set of segmented
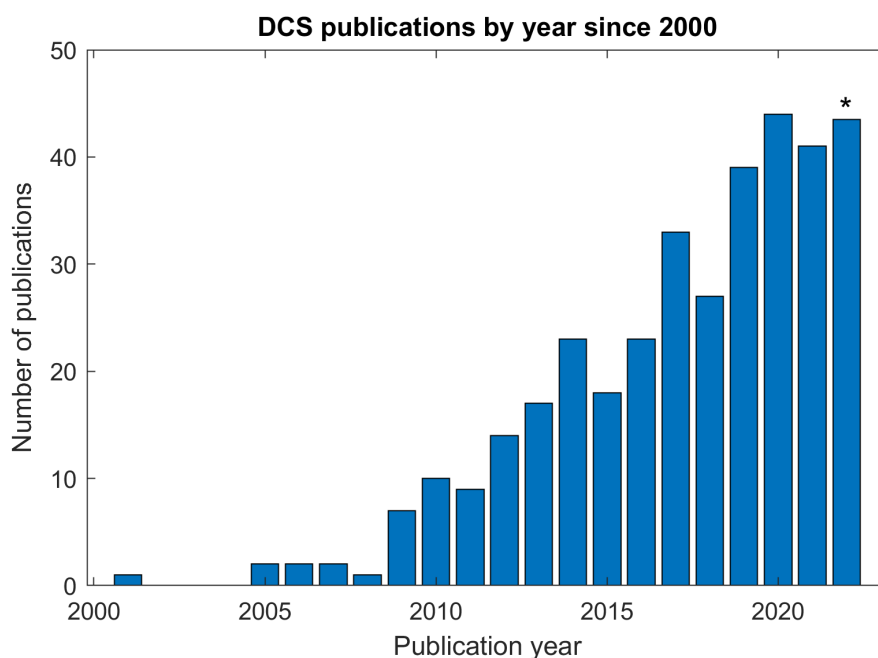

Fig. 1 Number of papers mentioning DCS in their title or abstract based on a PUBMED search (*value for 2022 extrapolated as of the date of writing).
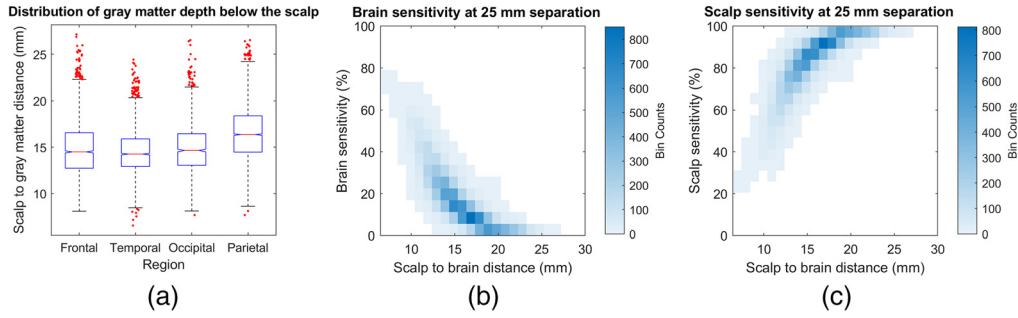
Fig. 2 Brain sensitivity evaluation for DCS at 25 mm source-detector separation. (a) Boxplot of distance between scalp and gray matter surface in different areas of the head (first, second (median), and third quartile range shown, with outliers defined as more than 2.67 standard deviations) from segmented MRI scans; (b) and (c) fraction of true change recovered from brain and superficial (scalp) tissue, respectively, as a function of the local distance between the scalp and gray matter surfaces.

MRI scans collected as part of a previous study (16 subjects, average age 29, range 25 to 41),[35] and subplots shown in Figs. 2(b) and 2(c) show the fractional recovery of a true blood flow change in the scalp and brain tissue, respectively, using simulation data from the same study[35] for the 25-mm source-detector separation used in the majority of published DCS investigations. As can be seen in these graphs, not only is the average brain sensitivity fairly low (on the order of 20% for typical scalp to brain distances in the frontal region for example), but the measurement has higher sensitivity to scalp than to brain blood flow. Of note, these results assume that the entire autocorrelation decay is being fitted. The early part of the decay is driven by photons that experience more scattering events, and thus it has higher CBF sensitivity; however, limiting the fit to the upper part of g_2 leads to significant increases in BF_i estimate variability and overall lower cerebral perfusion measurement SNR (see Supplementary Material in Ref. 36).

The noise performance versus cerebral sensitivity trade-off for DCS is in fact perhaps the biggest challenge to the wider adoption of this technology. Figure 3 displays the achievable data acquisition rate for a unitary contrast to noise ratio (CNR) and the relative brain to scalp sensitivity for DCS measurements at a range of source-detector separations between 5 and 40 mm.
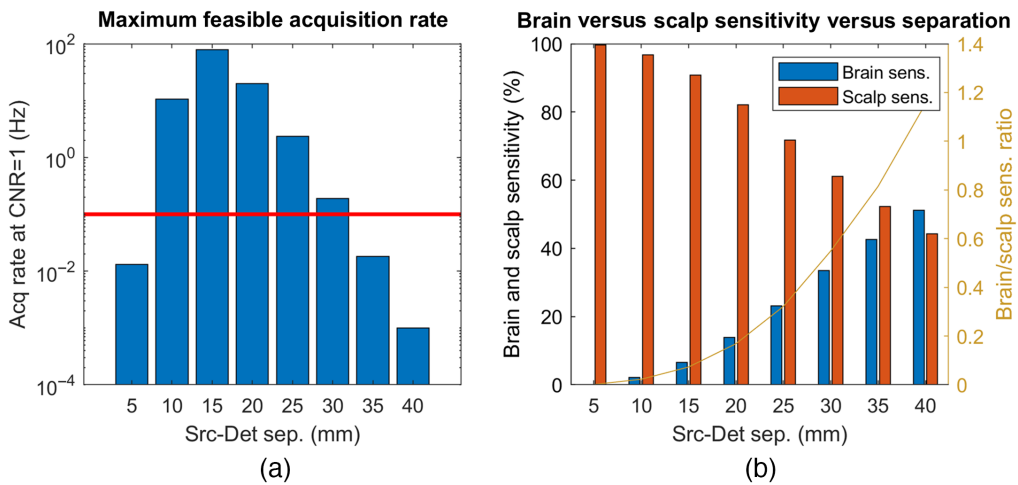

Fig. 3 Monte Carlo simulation-driven exploration of DCS measurement noise performance and cerebral versus extracerebral sensitivity: (a) achievable acquisition rates at unitary CNR, for typical DCS measurements at 850 nm across different source-detector separations (horizontal red line drawn at 0.1 Hz) with CNR defined as the fraction of the true cerebral perfusion change recovered by the DCS measurement divided by the standard deviation of the BFi estimate and (b) corresponding brain and scalp flow change fractional sensitivities versus separation.

These results are derived from Monte Carlo simulations on a simplified two layer slab geometry with a 12-mm superficial layer thickness (a somewhat conservative assumption in light of the actual scalp to brain distances shown in Fig. 2), assuming the same optical properties as Ref. 35 and photon count rates typical of our experimental data (11 kcps at 25 mm, scaled across other distances based on light fluence estimations). A step change in CBF was simulated versus baseline conditions, and CNR was defined as the fraction of the true cerebral perfusion change recovered using DCS measurements (under a homogeneous medium assumption) divided by the standard deviation of the BF_i estimate.

As seen in Fig. 3(a), the best CNR for CBF monitoring (notwithstanding physiological noise) is actually found at short separations, but at those distances there is little brain sensitivity, especially compared with scalp sensitivity. In contrast, the longest source-detector separation in which measurements are feasible with a reasonable integration time (less than 10 s, shown with a red line in Fig 3(a)) is ∼30 mm. However, even at 30 mm, we remain more sensitive to scalp than brain physiology.

Recently, excitement has been building toward the use of DCS for applications beyond baseline physiology monitoring, specifically for functional brain activation[37–40] and to assess the critical closing pressure of cerebral vasculature[41–43], a close surrogate of intracranial pressure with substantial clinical significance. However, these applications demand high data acquisition rates to resolve fast flow dynamics, including the detailed pulsatile flow shape.

Active technical development in the DCS field is thus focused on improving measurement SNR and increasing the fidelity of brain and other deep tissue perfusion measurement in conjunction with novel modeling and data processing algorithms, as well as on reducing the cost burden of implementing blood flow monitoring instrumentation.

3 Directions of Technical Development

3.1 Hardware Approaches for SNR/Depth Sensitivity Improvement

3.1.1 Multi-source and parallel detection DCS

The simplest approach to increasing DCS measurement SNR is increasing the amount of light delivered to the tissue as SNR is directly proportional to the photon counting rate.[44] The maximum permissible exposure is limited by safety standards (ANSI Z136.1 in the United States); however, two illumination positions separated by ∼5 mm can fit in most DCS probe designs, or simply a large spot (5 mm or larger) can be used, though it potentially makes short separation measurements more difficult. Additionally, multiple photon counting detection channels can be used to sample multiple speckles, as first demonstrated by Dietsche et al.[45] and further advanced by the availability of SPAD cameras with 1024 or more channels.[46,47] However, this approach has a high cost, and the improvement scales only with the square root of the detector channel number.

3.1.2 Heterodyne/interferometric detection

Another major avenue for increasing both the noise performance and the robustness of DCS measurements is the addition of a reference arm to achieve heterodyne interferometric detection, in which some of the source light is recombined with the photons collected from the tissue before the detector. For a standard DCS setup, conversion to heterodyne measurement doubles the SNR of the autocorrelation measurement and increases the SNR of the BF_i time course even more, especially at large source-detector separations.[48] Further, the measurement becomes substantially insensitive to environmental light, a significant advantage for practical use cases. By shifting the measured signal to a high intensity level, another important advantage of heterodyne detection is enabling the use of lower cost, noisier devices, and making it possible to use non-photon counting detectors, such as complementary metal-oxide-semiconductor (CMOS) cameras, as further detailed below. One downside is the stricter stability requirement for the laser source as directly coupled light dominates the detected signal.

3.1.3 *Multispeckle camera-based methods*

An alternative approach to multispeckle detection that is gaining increasing interest in the field is the use of low(er) cost CMOS cameras as massively parallel detector arrays. This has been demonstrated in the temporal domain, using a high-speed line scan cameras in conjunction with heterodyne detection to sample light collected by a multimode fiber;[49] in the Fourier domain, using heterodyne holographic demodulation across multiple speckles;[50] and in the spatial domain, imaging the speckle pattern collected at some distance away from the illumination location both without and with the use of a reference arm (termed speckle contrast optical spectroscopy,[51] and interferometric speckle visibility spectroscopy,[52] or multiexposure interferometric diffusing wave spectroscopy,[53] respectively). These approaches can exceed the performance of standard DCS even without the reference arm and can offer nearly two orders of magnitude improvement in the interferometric version, though the use of multimode detection fibers may increase sensitivity to motion artifacts.

3.1.4 *Long pathlength photon selection*

To improve sensitivity to flow in deep tissues, a number of methods have been proposed to isolate the photons that travel at depth and reject those that only probe superficial tissues. These include time-of-flight selection (time-resolved/time-domain DCS[54] and the related iNIRS technique[55]), pathlength selection through coherence gating,[56] and acoustic (ultrasound) tagging.[57,58] A major advantage of these techniques is that large source-detector separations are no longer needed, enabling compact probe design and/or dense spatial sampling and increased resolution, for example, for functional brain imaging. Further, time-domain DCS and iNIRS intrinsically sample the optical properties of the sample as well, providing both spectroscopic and flow property measurement.

3.1.5 *Long wavelength operation*

As DCS is based on light scattering, it has recently been shown that substantial benefits accrue from operating at longer wavelengths in the water absorption local minimum between 1050 and 1100 nm and in particular at 1064 nm, where there is a wide availability of optoelectronic components, including high power laser sources, which were initially developed for the telecom industry.[59] Due to increased skin exposure limits, slower autocorrelation decay, lower scattering, and lower energy per photon, an order of magnitude improvement is available in DCS measurement SNR. However, the lack of suitable semiconductor photon counting detectors represents a significant challenge, and initial demonstrations have used superconducting nanowire devices that are cryocooled and hence expensive and noisy.[60,61]

3.1.6 *Summary*

DCS and related techniques are the focus of intense technical development activities as described above and summarized in Table 1. Many of these approaches can potentially be combined to compound benefits, and several orders of magnitude improvements in SNR are likely; this can translate to faster acquisition rates and/or the ability to conduct measurements at larger source-detector separations with higher brain sensitivity.

3.2 *Advanced light Transport Modeling and Calibration Maneuvers*

Inspired by efforts in the NIRS community, advanced multilayer correlation transport models have been developed for DCS, using both analytical[38,62,63] and Monte Carlo simulation-based[64,65] approaches. By leveraging the differential depth sensitivity of the different regions of the autocorrelation curve, generally augmented by multidistance measurements, these methods seek to separately estimate superficial versus deep tissue blood flow. Several studies have reported the successful recovery of cerebral perfusion changes in the presence of extracerebral contamination during physiological maneuvers, such as hypercapnia.[36,66]

Table 1 Summary of technical development avenues for improving DCS SNR and depth sensitivity.

Method	Benefits
Parallel illumination and detection	SNR increase proportional to source power and to the square root of the number of detector channels.
Heterodyne/interferometric detection	Doubling of autocorrelation SNR allows for the use of low-cost, higher noise detectors, and robustness against environmental light conditions.
Multi-speckle camera-based detection	Substantial SNR benefit due to sampling large numbers of speckles, especially in conjunction with heterodyne detection.
Long pathlength photon selection	Increased depth sensitivity, independence of source-detector separation and thus higher spatial resolution for tomography.
Long wavelength operation	Substantial increase in available photon throughput and thus measurement SNR, availability of high power sources.

A downside of this approach is the increase in estimated BF_i time course noise due to limited cerebral perfusion sensitivity. Further, setting the appropriate geometry of the modeled layers can be challenging, even if structural medical imaging scans are available, because the Monte Carlo model fidelity is not sufficient to allow for the direct use of segmented anatomical information.[36] To aid in the selection of model parameters, the use of pressure modulation maneuvers was pioneered by Mesquita and Baker,[67,68] based on the principle that superficial perfusion perturbations should only impact scalp flow estimates, and brain BF_i should remain constant during the pressure period if layer thicknesses are chosen appropriately.

4 Future Perspective

We are in an exciting time in the development of noninvasive deep tissue perfusion monitoring technology. DCS and related approaches offer substantial promise in becoming a useful tool for both clinical decision making and functional imaging studies. The basic technology is proven, and the great progress being made in advancing measurement SNR, depth sensitivity, and robustness is likely to bear fruit in the near future. To this end, a focused effort is needed to convert the advances outlined in the previous section into reliable, compact, and easy to use instrumentation that can be brought into clinical spaces and operated by nonexperts.

At the crux of these translational efforts remains the need to ensure measurement accuracy, and, especially for clinical translation, the need to make the BF_i values interpretable.

Accuracy can be maximized using real-time evaluation criteria at the beginning of a measurement to ensure good brain sensitivity (such as comparing pressure modulation effects at short versus long separations, seeking locations where long channels display higher BF_i values than short channels, using any existing CT or MRI scan to plan probe placement, etc.) in conjunction with multilayer modeling to remove superficial physiology contamination—a task made feasible by leveraging hardware advances that increase both measurement SNR and brain sensitivity.

In parallel, there is a need to go beyond trend monitoring, toward being able to provide absolute perfusion values and establishing normative ranges that can be used in medical decision making. Efforts to calibrate BF_i are already ongoing in the field,[19,21,69] but it remains necessary to augment these not just with accurate measurement models as described above but also with validation studies to demonstrate that calibrated DCS perfusion values in clinician familiar units of flow/volume (mL of blood/mL of tissue/second) track those from established MRI and CT perfusion quantification methods in humans.

Last, but not least, there is a need for advances to enable the development of wearable, low-cost DCS devices not only to increase the dissemination of the technology but also to enable studies in naturalistic environments, akin to the developments in the fNIRS field.[70]

Disclosures

Acknowledgments

References

1. H. Ayaz et al., "Optical imaging and spectroscopy for the study of the human brain: status report," *Neurophotonics* **9**(Suppl 2), S24001 (2022).
2. T. Durduran et al., "Diffuse optics for tissue monitoring and tomography," *Rep. Prog. Phys.* **73**(7), 076701 (2010).
3. B. J. Berne and R. Pecora, *Dynamic Light Scattering*, Dover Publications, Inc., Mineola, New York (2000).
4. D. A. Boas, L. E. Campbell, and A. G. Yodh, "Scattering and imaging with diffusing temporal field correlations," *Phys. Rev. Lett.* **75**(9), 1855–1858 (1995).
5. C. Cheung et al., "In vivo cerebrovascular measurement combining diffuse near-infrared absorption and correlation spectroscopies," *Phys. Med. Biol.* **46**(8), 2053–2065 (2001).
6. H. L. Goldsmith and J. C. Marlow, "Flow behavior of erythrocytes. II. Particle motions in concentrated suspensions of ghost cells," *J. Colloid Interface Sci.* **71**(2), 383–407 (1979).
7. D. A. Boas et al., "Establishing the diffuse correlation spectroscopy signal relationship with blood flow," *Neurophotonics* **3**(3), 031412 (2016).
8. E. Sathialingam et al., "Hematocrit significantly confounds diffuse correlation spectroscopy measurements of blood flow," *Biomed. Opt. Express* **11**(8), 4786–4799 (2020).
9. S. Sakadzic, D. A. Boas, and S. Carp, "Theoretical model of blood flow measurement by diffuse correlation spectroscopy," *J. Biomed. Opt.* **22**(2), 027006 (2017).
10. V. N. Du Le and V. J. Srinivasan, "Beyond diffuse correlations: deciphering random flow in time-of-flight resolved light dynamics," *Opt. Express* **28**(8), 11191–11214 (2020).
11. S. A. Carp et al., "Validation of diffuse correlation spectroscopy measurements of rodent cerebral blood flow with simultaneous arterial spin labeling MRI; towards MRI-optical continuous cerebral metabolic monitoring," *Biomed. Opt. Express* **1**(2), 553–565 (2010).
12. T. Durduran et al., "Optical measurement of cerebral hemodynamics and oxygen metabolism in neonates with congenital heart defects," *J. Biomed. Opt.* **15**(3), 037004 (2010).
13. G. Yu et al., "Validation of diffuse correlation spectroscopy for muscle blood flow with concurrent arterial spin labeled perfusion MRI," *Opt. Express* **15**(3), 1064–1075 (2007).
14. C. Zhou et al., "Diffuse optical monitoring of hemodynamic changes in piglet brain with closed head injury," *J. Biomed. Opt.* **14**(3), 034015 (2009).
15. E. M. Buckley et al., "Cerebral hemodynamics in preterm infants during positional intervention measured with diffuse correlation spectroscopy and transcranial Doppler ultrasound," *Opt. Express* **17**(15), 12571–12581 (2009).
16. N. Roche-Labarbe et al., "Noninvasive optical measures of CBV, StO(2), CBF index, and rCMRO(2) in human premature neonates' brains in the first six weeks of life," *Hum. Brain Mapp.* **31**(3), 341–352 (2010).
17. M. N. Kim et al., "Noninvasive measurement of cerebral blood flow and blood oxygenation using near-infrared and diffuse correlation spectroscopies in critically brain-injured adults," *Neurocrit. Care* **12**(2), 173–180 (2010).
18. M. Diop et al., "Calibration of diffuse correlation spectroscopy with a time-resolved near-infrared technique to yield absolute cerebral blood flow measurements," *Biomed. Opt. Express* **2**(7), 2068–2081 (2011).

19. L. He et al., "Noninvasive continuous optical monitoring of absolute cerebral blood flow in critically ill adults," *Neurophotonics* **5**(4), 045006 (2018).

20. V. Jain et al., "Cerebral oxygen metabolism in neonates with congenital heart disease quantified by MRI and optics," *J. Cereb. Blood Flow Metab.* **34**(3), 380–388 (2014).

21. M. Giovannella et al., "Validation of diffuse correlation spectroscopy against (15)O-water PET for regional cerebral blood flow measurement in neonatal piglets," *J. Cereb. Blood Flow Metab.* **40**(10), 2055–2065 (2020).

22. T. Durduran and A. G. Yodh, "Diffuse correlation spectroscopy for non-invasive, micro-vascular cerebral blood flow measurement," *NeuroImage* **85**(Pt 1), 51–63 (2014).

23. D. Grosenick et al., "Review of optical breast imaging and spectroscopy," *J. Biomed. Opt.* **21**(9), 091311 (2016).

24. H. S. Yazdi et al., "Mapping breast cancer blood flow index, composition, and metabolism in a human subject using combined diffuse optical spectroscopic imaging and diffuse correlation spectroscopy," *J. Biomed. Opt.* **22**(4), 045003 (2017).

25. Y. Shang, K. Gurley, and G. Yu, "Diffuse correlation spectroscopy (DCS) for assessment of tissue blood flow in skeletal muscle: recent progress," *Anat. Physiol.* **3**(2), 128 (2013).

26. C. G. Bangalore-Yogananda et al., "Concurrent measurement of skeletal muscle blood flow during exercise with diffuse correlation spectroscopy and Doppler ultrasound," *Biomed. Opt. Express* **9**(1), 131–141 (2018).

27. V. Quaresima et al., "Diffuse correlation spectroscopy and frequency-domain near-infrared spectroscopy for measuring microvascular blood flow in dynamically exercising human muscles," *J. Appl. Physiol.* **127**(5), 1328–1337 (2019).

28. E. Sathialingam et al., "Small separation diffuse correlation spectroscopy for measurement of cerebral blood flow in rodents," *Biomed. Opt. Express* **9**(11), 5719–5734 (2018).

29. A. R. Ramirez et al., "Chemotherapeutic drug-specific alteration of microvascular blood flow in murine breast cancer as measured by diffuse correlation spectroscopy," *Biomed. Opt. Express* **7**(9), 3610–3630 (2016).

30. B. Rinehart, C. S. Poon, and U. Sunar, "Quantification of perfusion and metabolism in an autism mouse model assessed by diffuse correlation spectroscopy and near-infrared spectroscopy," *J. Biophotonics* **14**(11), e202000454 (2021).

31. R. C. Mesquita et al., "Tumor blood flow differs between mouse strains: consequences for vasoresponse to photodynamic therapy," *PLoS One* **7**(5), e37322 (2012).

32. C. Huang et al., "Speckle contrast diffuse correlation tomography of cerebral blood flow in perinatal disease model of neonatal piglets," *J. Biophotonics* **14**(4), e202000366 (2021).

33. B. R. White et al., "Low frequency power in cerebral blood flow is a biomarker of neurologic injury in the acute period after cardiac arrest," *Resuscitation* **178**, 12–18 (2022).

34. D. J. Pine et al., "Diffusing wave spectroscopy," *Phys. Rev. Lett.* **60**(12), 1134–1137 (1988).

35. M. M. Wu et al., "Complete head cerebral sensitivity mapping for diffuse correlation spectroscopy using subject-specific magnetic resonance imaging models," *Biomed. Opt. Express* **13**(3), 1131–1151 (2022).

36. M. M. Wu et al., "Improved accuracy of cerebral blood flow quantification in the presence of systemic physiology cross-talk using multi-layer Monte Carlo modeling," *Neurophotonics* **8**(1), 015001 (2021).

37. T. Durduran et al., "Diffuse optical measurement of blood flow, blood oxygenation, and metabolism in a human brain during sensorimotor cortex activation," *Opt. Lett.* **29**(15), 1766–1768 (2004).

38. J. Li et al., "Noninvasive detection of functional brain activity with near-infrared diffusing-wave spectroscopy," *J. Biomed. Opt.* **10**(4), 044002 (2005).

39. N. Roche-Labarbe et al., "Somatosensory evoked changes in cerebral oxygen consumption measured non-invasively in premature neonates," *NeuroImage* **85**(Pt 1), 279–286 (2014).

40. C. Poon et al., "Cerebral blood flow-based resting state functional connectivity of the human brain using optical diffuse correlation spectroscopy," *J. Vis. Exp* (159), e60765 (2020).

41. W. B. Baker et al., "Noninvasive optical monitoring of critical closing pressure and arteriole compliance in human subjects," *J. Cereb. Blood Flow Metab.* **37**(8), 2691–2705 (2017).

42. K. C. Wu et al., "Validation of diffuse correlation spectroscopy measures of critical closing pressure against transcranial Doppler ultrasound in stroke patients," *J. Biomed. Opt.* **26**(3), 036008 (2021).

43. J. B. Fischer et al., "Non-invasive estimation of intracranial pressure by diffuse optics: a proof-of-concept study," *J. Neurotrauma* **37**(23), 2569–2579 (2020).

44. D. E. Koppel, "Statistical accuracy in fluorescence correlation spectroscopy," *Phys. Rev. A* **10**(6), 1938–1945 (1974).

45. G. Dietsche et al., "Fiber-based multispeckle detection for time-resolved diffusing-wave spectroscopy: characterization and application to blood flow detection in deep tissue," *Appl. Opt.* **46**(35), 8506–8514 (2007).

46. W. Liu et al., "Fast and sensitive diffuse correlation spectroscopy with highly parallelized single photon detection," *APL Photonics* **6**(2), 026106 (2021).

47. E. J. Sie et al., "High-sensitivity multispeckle diffuse correlation spectroscopy," *Neurophotonics* **7**(3), 035010 (2020).

48. M. Robinson et al., "Interferometric diffuse correlation spectroscopy improves measurements at long source-detector separation and low photon count rate," *J. Biomed. Opt.* **25**(9), 097004 (2020).

49. W. Zhou et al., "Functional interferometric diffusing wave spectroscopy of the human brain," *Sci. Adv.* **7**(20), eabe0150 (2021).

50. E. James and S. Powell, "Fourier domain diffuse correlation spectroscopy with heterodyne holographic detection," *Biomed. Opt. Express* **11**(11), 6755–6779 (2020).

51. C. P. Valdes et al., "Speckle contrast optical spectroscopy, a non-invasive, diffuse optical method for measuring microvascular blood flow in tissue," *Biomed. Opt. Express* **5**(8), 2769–2784 (2014).

52. J. Xu et al., "Interferometric speckle visibility spectroscopy (ISVS) for human cerebral blood flow monitoring," *APL Photonics* **5**(12), 126102 (2020).

53. W. Zhou et al., "Multi-exposure interferometric diffusing wave spectroscopy," *Opt. Lett.* **46**(18), 4498–4501 (2021).

54. J. Sutin et al., "Time-domain diffuse correlation spectroscopy," *Optica* **3**(9), 1006–1013 (2016).

55. O. Borycki et al., "Interferometric near-infrared spectroscopy (iNIRS) for determination of optical and dynamical properties of turbid media," *Opt. Express* **24**(1), 329–354 (2016).

56. A. M. Safi et al., "Quantitative measurement of static and dynamic tissue optical properties with continuous wave pathlength resolved diffuse correlation spectroscopy," in *Biophotonics Congr. 2021, OSA Technical Digest*, E. Buckley, Ed., Optica Publishing Group, Washington, DC, p. BTh1B.6 (2021).

57. A. Tsalach et al., "Ultrasound modulated light blood flow measurement using intensity autocorrelation function: a Monte-Carlo simulation," *Proc. SPIE* **8943**, 89433N (2014).

58. M. B. Robinson et al., "Characterization of continuous wave ultrasound for acousto-optic modulated diffuse correlation spectroscopy (AOM-DCS)," *Biomed. Opt. Express* **11**(6), 3071–3090 (2020).

59. S. Carp et al., "Diffuse correlation spectroscopy measurements of blood flow using 1064 nm light," *J. Biomed. Opt.* **25**(9), 097003 (2020).

60. N. Ozana et al., "Superconducting nanowire single-photon sensing of cerebral blood flow," *Neurophotonics* **8**(3), 035006 (2021).

61. N. Ozana et al., "Functional time domain diffuse correlation spectroscopy," *Front. Neurosci.* **16**, 932119 (2022).

62. W. B. Baker et al., "Modified Beer-Lambert law for blood flow," *Biomed Opt Express* **5**(11), 4053–4075 (2014).

63. L. Gagnon et al., "Investigation of diffuse correlation spectroscopy in multi-layered media including the human head," *Opt. Express* **16**(20), 15514–15530 (2008).

64. D. A. Boas, *Diffuse Photon Probes of Structural and Dynamical Properties of Turbid Media: Theory and Biomedical Applications*, Physics: University of Pennsylvania; 1996.

65. J. Selb et al., "Sensitivity of near-infrared spectroscopy and diffuse correlation spectroscopy to brain hemodynamics: simulations and experimental findings during hypercapnia," *Neurophotonics* **1**(1), 015005 (2014).

66. D. Milej et al., "Direct assessment of extracerebral signal contamination on optical measurements of cerebral blood flow, oxygenation, and metabolism," *Neurophotonics* **7**(4), 045002 (2020).

67. R. C. Mesquita et al., "Influence of probe pressure on the diffuse correlation spectroscopy blood flow signal: extra-cerebral contributions," *Biomed. Opt. Express* **4**(7), 978–994 (2013).

68. W. B. Baker et al., "Pressure modulation algorithm to separate cerebral hemodynamic signals from extracerebral artifacts," *Neurophotonics* **2**(3), 035004 (2015).

69. M. Khalid et al., "Development of a stand-alone DCS system for monitoring absolute cerebral blood flow," *Biomed. Opt. Express* **10**(9), 4607–4620 (2019).

70. P. Pinti et al., "A review on the use of wearable functional near-infrared spectroscopy in naturalistic environments," *Jpn. Psychol. Res.* **60**(4), 347–373 (2018).

Stefan Carp, PhD is an assistant professor of radiology at Harvard Medical School and a member of the MGH Martinos Center Optics Group. He received his BS degrees in Chemistry and Chemical Engineering from MIT and a PhD from the University of California, Irvine, in biomedical optics. His interests are in advancing technologies for noninvasive optical monitoring of tissue hemodynamics and in collaborating with physicians to explore their clinical translation to improve patient outcomes.

Mitchell B. Robinson, PhD, is currently a postdoctoral research fellow at the Athinoula A. Martinos Center for Biomedical Imaging at Massachusetts General Hospital. He is a graduate of the Harvard-MIT Program in Health Sciences and Technology in 2022. His research interests include the development of modifications to diffuse optical methods, most recently applied to diffuse correlation spectroscopy, and their application to clinical blood flow monitoring.

Maria A. Franceschini, PhD, is a professor at Harvard Medical School with specific training and expertise in the development of noninvasive optical techniques and applications in neuro-science, neurology, and brain health. As a pioneer in the fields of NIRS and DCS, she has made substantial contributions to the development of advanced near-infrared optical monitoring instruments, and she has successfully applied these technologies to a large range of functional neuroimaging and clinical neuromonitoring applications.